



The diagnostic value of contrast-enhanced ultrasound combined with clinicopathological features in microinvasive ductal carcinoma *in situ*

Ying Jiang^{1,2}, Jun-Kang Li¹, Si-Si Huang¹, Shi-Yu Li¹, Rui-Lan Niu¹, Nai-Qin Fu¹, Zhi-Li Wang¹

¹Department of Ultrasound, Chinese People's Liberation Army General Hospital, Beijing, China; ²Department of Ultrasound, The Affiliated Hospital of Inner Mongolia Medical University, Huhhot, China

Contributions: (I) Conception and design: Y Jiang, ZL Wang; (II) Administrative support: None; (III) Provision of study materials or patients: JK Li, SY Li; (IV) Collection and assembly of data: None; (V) Data analysis and interpretation: Y Jiang, SS Huang; (VI) Manuscript writing: All authors; (VII) Final approval of manuscript: All authors.

Correspondence to: Zhi-Li Wang, MD. Department of Ultrasound, Chinese People's Liberation Army General Hospital, 28 Fuxing Road, Beijing 100853, China. Email: wzllg@sina.com.

Background: Ductal carcinoma in situ with microinvasion (DCISM) represents 1% of all breast cancer cases and is arguably a more aggressive subtype of ductal carcinoma in situ (DCIS). Preoperative evaluation of DCISM usually relies on core needle biopsy, and non-invasive evaluation methods are relatively limited. This study aims to explore the features of conventional ultrasound (US) and contrast-enhanced ultrasound (CEUS) in DCISM and to analyze the US and clinicopathological predictors of infiltrating components.

Methods: A retrospective collection of US, CEUS, and clinicopathologic data for DCIS and DCISM lesions was conducted from January 1, 2019 to June 30, 2022. The Breast Imaging Reporting and Data System (BI-RADS) criteria were used to evaluate breast lesions. On CEUS, the imaging features were scored using a 5-point scoring system to re-rate the BI-RADS category indicated by conventional US features. The pathological diagnosis served as the gold standard. Histopathologic features included comedo-type necrosis and pathological grade, while biomarkers included estrogen receptor (ER), progesterone receptor (PR), human epidermal growth factor receptor 2 (HER2), and the Ki-67 index. A logistic regression analysis was performed to identify the independent risk factors for DCISM. The diagnostic performance of the model was evaluated using the receiver operating characteristic (ROC) curve and calculating the area under the curve (AUC).

Results: A total of 89 women were included in the study. Of these, 66 had a pathologic diagnosis of DCIS (66 lesions, ranging in size from 0.6 to 4.9 cm), and 23 had a pathologic diagnosis of DCISM (23 lesions, ranging in size from 0.7 to 4.2 cm). Three features on conventional US (tumor size, margin, and calcification) and three enhancement features on CEUS (enhancement margin, enhancement mode, and enhancement scope) were found to be significantly different between the DCIS and DCISM lesions ($P=0.03$, $P=0.04$, $P=0.02$, $P=0.03$, $P=0.03$, $P=0.007$, respectively). Patients with DCISM were more likely to have a higher pathological grade, ER negativity, PR negativity, HER2 positivity, and a higher Ki-67 index than patients with DCIS ($P<0.001$, $P=0.042$, $P=0.03$, $P=0.009$, $P=0.05$, respectively). A multivariate logistic regression analysis further showed that only an enlarged enhancement scope and pathological grade were associated with DCISM. The sensitivity and specificity of this predictive model were 87.0% and 81.8%, respectively (AUC =0.89). The absence of calcifications, non-mass lesions, lack of vascularity, and the non-enlarged scope can lead to misdiagnosis of DCIS and DCISM.

Conclusions: Understanding the CEUS and clinicopathologic features of DCISM lesions may alert clinicians to the possibility of microinvasion and guide appropriate management.

Keywords: Ductal carcinoma in situ with microinvasion (DCISM); contrast-enhanced ultrasound (CEUS); misdiagnosis

Submitted May 31, 2024. Accepted for publication Oct 11, 2024. Published online Nov 26, 2024.

doi: 10.21037/gs-24-211

View this article at: <https://dx.doi.org/10.21037/gs-24-211>

Introduction

Breast cancer is one of the most common malignant tumors in women. Among them, breast ductal carcinoma in situ (DCIS) is a tumorous lesion where abnormal cell accumulation is confined to the basement membrane of the duct wall and does not invade the surrounding matrix (1,2). DCIS with microinvasion (DCISM) is a subtype of DCIS and accounts for approximately 1% of breast cancers (3). DCISM is more aggressive than DCIS, and patients with DCISM tend to have poorer cancer-specific and overall survival rates (4). Therefore, an accurate diagnosis distinguishing DCISM from DCIS is essential for optimal treatment and improved clinical outcomes. Preoperative assessment of DCISM can be performed by core needle biopsy. However, previous studies have shown that 15–20% of patients initially diagnosed with DCIS by core needle biopsy are found to have upstaged to invasive disease at the time of surgical excision (5-7). Currently, there is a lack of recognized, non-invasive assessment modalities that are valid for diagnosing DCISM. In China, more than 75% of women in the breast category are classified as the dense type (8). Mammography methods have limited efficacy in

women with dense breasts. The wide availability, low cost, and safety of ultrasound (US) has become an important screening tool for the evaluation of breast lesions. At present, it has been confirmed that deep learning can be used to identify microscopic infiltrates of breast DCIS from US images (9). Contrast-enhanced ultrasound (CEUS) is a leading technique that can be used to assess blood distribution and provide qualitative and quantitative analyses of breast lesion characteristics, but it is unclear whether CEUS is beneficial in the diagnosis of DCIS and DCISM. In this study, we retrospectively analyzed the clinicopathological features and US image characteristics of patients with surgical pathology diagnosed with DCIS and DCISM. We explored the relationship between the clinicopathological features and imaging manifestations of DCISM to enhance our understanding of its biological behavior and imaging characteristics. This research aims to provide more pathological and imaging evidence for personalized treatment and prognostic judgment in clinical practice. We present this article in accordance with the STARD reporting checklist (available at <https://gs.amegroups.com/article/view/10.21037/gs-24-211/rc>).

Methods

Patients

The study was conducted in accordance with the Declaration of Helsinki (as revised in 2013). The study was a retrospective clinical diagnostic test, approved by the Ethics Committee of the Chinese PLA General Hospital (No. S2020-354-01). Informed consent was waived because of the retrospective nature of the study. A retrospective search was performed for all breast lesions from January 1, 2019 to June 30, 2022 at the General Hospital of the Chinese People's Liberation Army of China. The inclusion criteria were as follows: (I) patients with intraductal papilloma lesions of the breast who underwent surgical resection and pathologic diagnosis of DCIS or DCISM; (II) patients with complete preoperative conventional US and CEUS data; (III) available clinical data. The exclusion criteria were as follows: (I) patients with other histological lesions in the same breast; (II) breast lesions that could not

Highlight box

Key findings

- Contrast-enhanced ultrasound (CEUS) combined with clinicopathologic features contributes to the diagnosis of ductal carcinoma in situ with microinvasion (DCISM).

What is known and what is new?

- Preoperative assessment of DCISM can be performed by core needle biopsy. Currently, there is a lack of recognized non-invasive assessment modalities that are valid for the diagnosis of DCISM.
- Our study demonstrated that imaging features from CEUS are helpful in the diagnosis of DCISM. Ductal carcinoma in situ (DCIS) and DCISM lesions are prone to be misdiagnosed when they exhibit no calcifications, non-mass lesions, or lack of blood flow signal, and a non-enlarged scope.

What is the implication, and what should change now?

- Our current findings may help predict the aggressiveness of DCIS cases, thereby enabling the development of more personalized management methods.

be accurately evaluated using conventional US and CEUS; (III) cases with only gross needle biopsy results and missing surgical specimen pathology.

US and CEUS examinations

US and CEUS examinations were performed with a Mindray Resona 7S (Mindray Medical International) using an L11-3 linear array probe with a frequency of 5.6–10.0 MHz. Patients were positioned lying flat or lateral supine position with elevation of both upper limbs. First, an US examination of the lesion was performed. The US features of the lesions were recorded. Identify the cut surface with the most abundant lesion blood flow signal before proceeding to the CEUS pattern. The double scope imaging was opened and the focus was adjusted to the posterior side of the lesion. After stabilizing the image, 5 mL SonoVue (Bracco company) was injected intravenously, followed by a bolus of 5 mL saline. Patients remained calm, breathing normally, as a dynamic contrast video was recorded for 3 minutes, and offline analysis was performed after storage.

Image analysis

Two physicians with more than five years of experience in breast US evaluated the images without prior knowledge of the clinical and histopathologic findings. The American College of Radiology 5th Edition Breast Imaging Reporting and Data System (BI-RADS) criteria were referenced for the evaluation of breast lesions (10). DCIS and DCISM lesions were described in terms of shape, tumor size, orientation, echogenicity, margin, vascularity, ductal extension, and evidence of microcalcification. On CEUS, enhancement patterns were described based on clinical experience and previous literature (11–13). Parameters evaluated for CEUS patterns of lesions included wash-in/wash-out times, enhancement margins, enhancement direction, enhancement intensity, enhancement mode, enhancement scope (an increase of ≥ 3 mm in length or width compared with values measured by conventional US was defined as an expanded range), and penetrating vessels. Then, according to the 5-point scoring system proposed by Xiao *et al.* (14), the imaging features on CEUS were scored to re-rate the BI-RADS category indicated by conventional US features. We determined diagnostic accuracy when the lesions of DCIS or DCISM were classified as BI-RADS categories 4b–5, and misdiagnosis was determined when the lesions of DCIS or DCISM were classified as BI-RADS 3–4a.

Histological analysis

All pathological diagnoses were independently evaluated and agreed upon by 2 pathologists with more than 5 years of experience. Histopathologic features included comedo-type necrosis and pathological grade, while biomarkers included estrogen receptor (ER), progesterone receptor (PR), human epidermal growth factor receptor 2 (HER2), and Ki-67 index. ER and PR positivity were defined as nuclear staining in 1% or more of tumor cells (15). HER2 expression 3+ by immunohistochemistry or fluorescence *in situ* hybridization showed HER2 gene amplification was considered positive. Ki-67 expression was quantified using a visual grading system. An estimated percentage of Ki-67 positive cells was determined, and the cutoff for positivity was established at 20% (16).

Statistical analysis

SPSS 25.0 software (SPSS, Chicago, IL, USA) was utilized for statistical analysis. Patients' age and maximum diameter of lesions were compared using the Mann-Whitney *U* test. US and CEUS characteristics, histopathologic characteristics were compared between the two groups of patients using χ^2 test and Fisher's exact test. Univariate analysis of variance and multivariate logistic regression analysis were used to determine the independent factors of DCISM. The diagnostic performance of the model was evaluated using the receiver operating characteristic (ROC) curve and calculating the area under the curve (AUC). $AUC \leq 0.5$ indicated that the model had no classification ability; $0.5 < AUC < 0.7$ indicated that the model had a certain classification ability; $0.7 \leq AUC < 0.9$ indicated that the model had good classification ability; $AUC \geq 0.9$ indicated that the model had very good classification ability. Two-sided *P* values of < 0.05 were considered indicative of statistically significant differences.

Results

The clinical and pathologic characteristics

During the 4-year study period, a total of 321 patients were identified. After excluding 198 patients with intraductal papilloma, 23 patients with missing CEUS data, and 11 patients without surgical pathology specimens. Eighty-nine patients, all female, were finally included in the study cohort (Figure 1). Group 1 consisted of 66 patients (66 lesions, with a mean size of 2.033 cm and a size range of 0.6–4.9 cm)

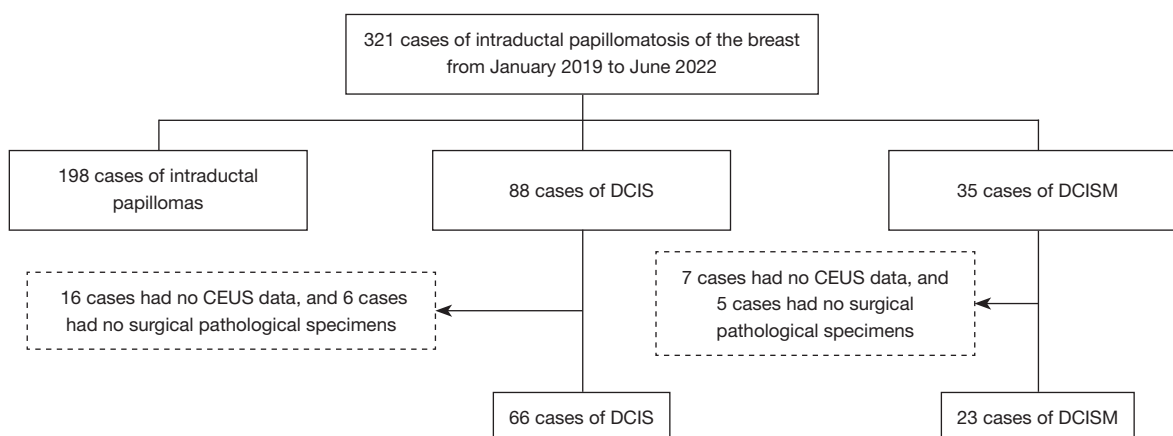


Figure 1 Flowchart of the selection of 89 patients. DCIS, ductal carcinoma in situ; DCISM, ductal carcinoma in situ with microinvasion; CEUS, contrast-enhanced ultrasound.

diagnosed with DCIS. The patients' ages ranged from 31 to 77 years, with a mean age of 48 years. Group 2 consisted of 23 patients (23 lesions, with a mean size of 2.244 cm and a size range of 0.7–4.2 cm) diagnosed of DCISM. The patients' ages ranged from 29 to 78 years, with a mean age 49 years. However, there was no significant difference in patients age between the two disease entities ($P=0.06$; *Table 1*). Patients with DCISM were more likely to have larger and higher pathological grade tumors, ER negativity, PR negativity, HER2 positivity, and a higher Ki-67 index than patients with DCIS ($P<0.001$, $P=0.042$, $P=0.03$, $P=0.009$, $P=0.050$, respectively; *Table 2*).

Sonographic features of DCIS and DCISM on conventional US and CEUS

As shown in *Table 1*, significant differences in the tumor size, margin, and calcification were observed between DCIS and DCISM ($P=0.03$, $P=0.04$, $P=0.02$, respectively). However, the shape, orientation, echogenicity, vascularity, and ductal extension of the lesions were not statistically significant ($P=0.07$, $P=0.57$, $P=0.89$, $P=0.88$, $P=0.26$, respectively). Tumor size <2.5 cm was more common in DCIS (69.7%, 46/66) than in DCISM (43.5%, 10/23). Regarding the margins, 69.7% (46/66) DCIS cases showed margins that were not circumscribed, while 91.3% (21/23) DCISM showed margins that were not circumscribed ($\chi^2=4.279$, $P=0.04$). In terms of calcification, the presence of calcification was more frequent in the DCISM (65.2%, 15/23) than in the DCIS (37.9%, 25/66). The cases of DCIS and DCISM were statistically different in three

enhancement features: enhancement margin, enhancement mode and enhancement scope ($P=0.03$, $P=0.03$, $P=0.007$, respectively; *Table 3*; *Figure 2*). Most of the DCISM lesions (11/23, 47.8%) showed unclear boundaries after enhancement, while a smaller proportion of DCIS lesions (16/66, 24.2%) showed blurred enhancement margin ($\chi^2=4.489$, $P=0.03$); 91.3% (21/23) of DCISM lesions had heterogeneous internal echogenicity after enhancement; in contrast, only 68.2% (45/66) of DCIS lesions presented this feature ($\chi^2=4.758$, $P=0.03$). The enlargement of scope was observed in 78.3% (18/23) of the DCISM lesions, whereas only 45.5% (30/66) of the DCIS lesions exhibited this feature ($\chi^2=7.388$, $P=0.007$). Other enhancement features, such as the wash-in time, enhancement direction, enhancement intensity, penetrating vessels, and wash-out time, did not show significant differences between the two groups ($P=0.65$, $P=0.52$, $P=0.86$, $P=0.50$, $P=0.17$, respectively).

Diagnostic value of logistic regression models

A logistic regression analysis was performed to identify the independent risk factors for DCISM. The candidate factors included the tumor size, margin, calcifications, enhancement margin, enhancement mode, enhancement scope, pathological grade, ER, PR, HER2 status, and Ki-67. All these factors were selected based on the univariate regression analysis. Finally, two indicators were identified as features that correlated with DCISM, including the pathological grade ($P=0.002$), enhancement scope ($P=0.01$; *Figure 3*). The ROC curves were plotted to assess

Table 1 Age distribution and traditional US characteristics of DCIS (n=66) and DCISM (n=23)

Characteristic	DCIS, n (%)	DCISM, n (%)	χ^2	P
Age			3.497	0.06
<45 years	32 (48.5)	6 (26.1)		
≥45 years	34 (51.5)	17 (73.9)		
Tumor size			5.026	0.03
<2.5 cm	46 (69.7)	10 (43.5)		
≥2.5 cm	20 (30.3)	13 (56.5)		
Shape			3.379	0.07
Mass	48 (72.7)	21 (91.3)		
Non-mass abnormality	18 (27.3)	2 (8.7)		
Orientation			-	0.57
Parallel	62 (93.9)	23 (100.0)		
Not parallel	4 (6.1)	0 (0.0)		
Echogenicity			0.476	0.89
Hypoechoic	41 (62.1)	14 (60.9)		
Isoechoic	2 (3.0)	0 (0.0)		
Hyperechoic	0 (0.0)	0 (0.0)		
Complex cystic and solid	23 (34.8)	9 (39.1)		
Margin			4.279	0.04
Circumscribed	20 (30.3)	2 (8.7)		
Not circumscribed	46 (69.7)	21 (91.3)		
Vascularity			0.022	0.88
Present	39 (59.1)	14 (60.9)		
Absent	27 (40.9)	9 (39.1)		
Ductal extension			1.293	0.26
Present	15 (22.7)	8 (34.8)		
Absent	51 (77.3)	15 (65.2)		
Calcifications			5.152	0.02
Present	25 (37.9)	15 (65.2)		
Absent	41 (62.1)	8 (34.8)		

US, ultrasound; DCIS, ductal carcinoma in situ; DCISM, ductal carcinoma in situ with microinvasion.

the performance of the risk factors and prediction model (Figure 4). The AUC using this predicting model was 0.892 [95% confidence interval (CI): 0.824–0.959]. The sensitivity and specificity were found to be 87.0% and 81.8%.

Analysis of misdiagnosed cases

Comparisons of original US BI-RADS scores and CEUS rerated BI-RADS scores with pathology results are shown in Table 4. On conventional US, 49.4% (44/89) of the

Table 2 Summary of histopathologic characteristics

Characteristic	DCIS, n (%)	DCISM, n (%)	χ^2	P
Comedo-type necrosis			0.465	0.50
Yes	18 (27.3)	8 (34.8)		
No	48 (72.7)	15 (65.2)		
Pathological grade			13.355	<0.001
Grade 1–2	46 (69.7)	6 (26.1)		
Grade 3	20 (30.3)	17 (73.9)		
Estrogen receptor			4.152	0.042
Positive	54 (81.8)	14 (60.9)		
Negative	12 (18.2)	9 (39.1)		
Progesterone receptor			4.940	0.03
Positive	55 (83.3)	14 (60.9)		
Negative	11 (16.7)	9 (39.1)		
HER2 status			9.283	0.009
0, 1+	12 (18.2)	7 (30.4)		
2+	35 (53.0)	4 (17.4)		
3+	19 (28.8)	12 (52.2)		
Ki-67 index (%)			3.844	0.050
<20	44 (66.7)	10 (43.5)		
≥20	22 (33.3)	13 (56.5)		

DCIS, ductal carcinoma in situ; DCISM, ductal carcinoma in situ with microinvasion; HER2, human epidermal growth factor receptor 2.

malignant lesions were classified as BI-RADS (3-4A). After CEUS evaluation, 28.1% (25/89) of the malignant lesions were diagnosed as BI-RADS (3-4A). A total of 25 cases were misdiagnosed after US and CEUS evaluation. All 89 cases were divided into correctly diagnosed (n=64) and misdiagnosed (n=25) groups. Among the misdiagnosed cases included 24 cases of DCIS and one case of DCISM. Chi-square analysis indicates that absence of calcifications, non-mass lesions, and lack of vascularity on conventional US and the absence of enlargement of the enhancement range may lead to an incorrect diagnosis of DCIS and DCISM (P=0.003, P=0.02, P=0.03, P<0.001, respectively; *Figure 5*). There was no significant difference in the tumor size, orientation, echogenicity, margin, ductal extension, wash-in time, enhancement margin, enhancement direction, enhancement intensity, enhancement mode, wash-out time of the mass (P=0.27, P=0.07, P=0.26, P=0.32, P=0.41, P=0.24, P=0.42, P=0.34 P=0.11, P=0.07, P=0.19, respectively).

Discussion

DCIS of the breast is early-stage breast cancer that refers to heavy atypical proliferative carcinomatosis of epithelial cells within the ductal and terminal lobular units of the breast, which has not invaded through the basement membrane of the duct wall nor the surrounding stroma (17). DCIS is a non-invasive form of breast cancer with a low mortality rate, so there is currently the potential for overtreatment, and several clinical trials are investigating whether the level of management can be reduced by actively monitoring low-risk DCIS by imaging means (18-21). The 5th edition of the American Joint Committee on Cancer manual published in 1997 officially defined DCISM as tumor cells breaking through the basement membrane and invading the surrounding tissue, but the maximum diameter of the invasive lesion does not exceed 1 mm, and classified it as T1mic stage (22). It is estimated that the incidence of lymph node metastasis in DCISM is 0–14% (3,21,23).

Table 3 Enhancement features on CEUS between DCIS (n=66) and DCISM (n=23)

Characteristic	DCIS, n (%)	DCISM, n (%)	χ^2	P
Wash-in time			1.133	0.65
Earlier	39 (59.1)	11 (47.8)		
Synchronous	24 (36.4)	11 (47.8)		
Later	3 (4.5)	1 (4.3)		
Enhancement margin			4.489	0.03
Clear	50 (75.8)	12 (52.2)		
Blurred	16 (24.2)	11 (47.8)		
Enhancement direction			1.587	0.52
Centripetal	21 (31.8)	8 (34.8)		
Centrifugal	4 (6.1)	3 (13.0)		
Diffuse	41 (62.1)	12 (52.2)		
Enhancement intensity			0.493	0.86
Hypo intensity	4 (6.1)	2 (8.7)		
Iso intensity	4 (6.1)	1 (4.3)		
Hyper intensity	58 (87.8)	20 (87.0)		
Enhancement mode			4.758	0.03
Homogeneous	21 (31.8)	2 (8.7)		
Heterogeneous	45 (68.2)	21 (91.3)		
Enhancement scope			7.388	0.007
Enlarged	30 (45.5)	18 (78.3)		
Not enlarged	36 (54.5)	5 (21.7)		
Penetrating vessels			0.465	0.50
Presence	18 (27.3)	8 (34.8)		
Absence	48 (72.7)	15 (65.2)		
Wash-out time			3.365	0.17
Earlier	1 (1.5)	1 (4.3)		
Synchronous	36 (54.5)	8 (34.8)		
Later	29 (43.9)	14 (60.9)		

CEUS, contrast-enhanced ultrasound; DCIS, ductal carcinoma in situ; DCISM, ductal carcinoma in situ with microinvasion.

CEUS is more sensitive in detecting angiogenesis than color Doppler flow imaging. But, the diagnosis of DCIS and DCISM by conventional US and CEUS has rarely been evaluated. In this study, the imaging features of DCIS and DCISM detected by conventional US and CEUS were evaluated and a prediction model based on these imaging features was established, which may help in predicting the

DCIS microinvasion. At the same time, we also analyzed the reasons for the misdiagnosis of DCIS and DCISM by US.

The DCISM group had larger lesions (≥ 2 cm) with relatively ill-defined borders (21/23, 91.3%) and was more likely to exhibit calcification (15/23, 65.2%). Jin *et al.* (24) retrospectively analyzed 129 patients with DCIS and found

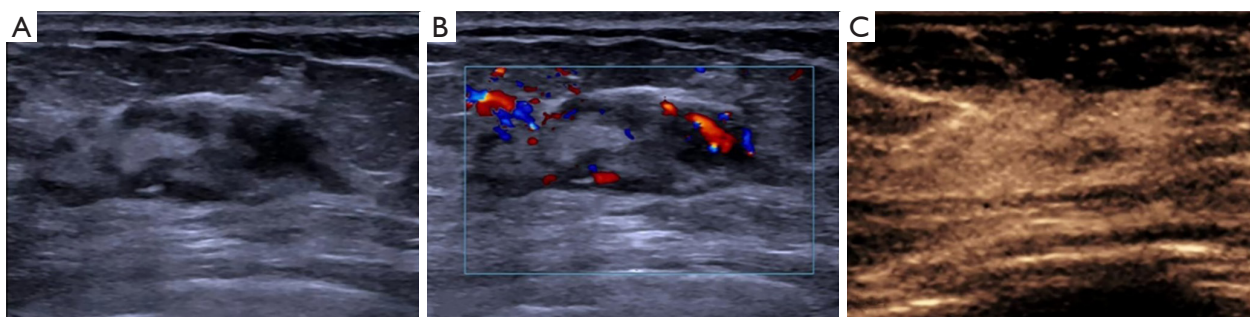


Figure 2 A 47-year-old woman with a pathologic DCISM. (A) Schematic diagram of conventional US. (B) Schematic diagram of color Doppler. (C) Schematic diagram of CEUS. DCISM, ductal carcinoma in situ with microinvasion; US, ultrasound; CEUS, contrast-enhanced ultrasound.

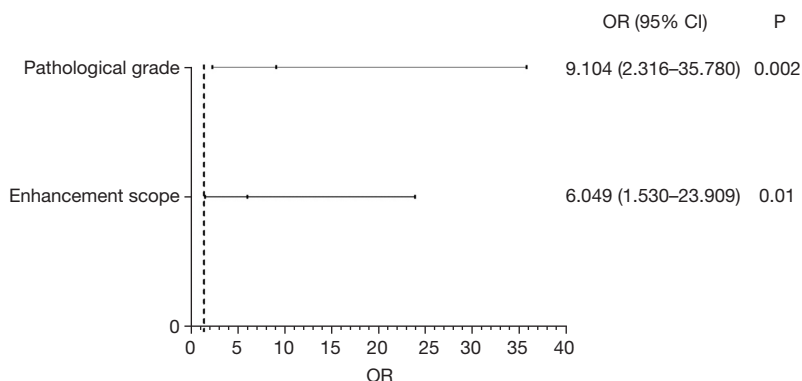


Figure 3 Multivariate logistic regression analysis for diagnosis of ductal carcinoma *in situ* with microinvasion. OR, odds ratio; CI, confidence interval.

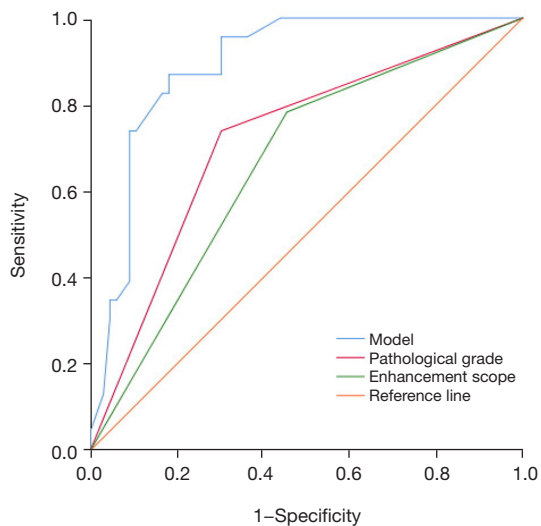


Figure 4 Logistic regression model to predict receiver operating characteristic curve for ductal carcinoma in situ with microinvasion.

that the incidence of microinvasion increased with the maximum diameter of the tumor. They also found that the correlation between tumor size and microinvasion assessed by US was higher than that obtained with mammography. Therefore, it is reasonable to assume that if a large area of the lesion is found on US, especially if multiple quadrants are involved, the possibility of the tumor with microinvasion increases. DCIS tumor cells are confined to ductal and lobular glandular lumina at an early stage, with intact basement membranes and mostly smooth margins. However, DCISM shows loss of basement membrane architecture with outward invasion of heterotypic cells, reactive proliferation, and traction of the surrounding connective tissue, which can easily develop sonographic features of marginal opacity. This explains why the borders of DCISM on US are relatively more ill-defined. Although sonography is less sensitive than mammography for the

Table 4 Comparison of original BI-RADS scores and CEUS rerated BI-RADS scores with pathology results

BI-RADS category	Rerated BI-RADS category	Pathology	
		DCIS (n=66)	DCISM (n=23)
3 (n=5)	3 (n=1)	1	0
	4A (n=3)	2	1
	4B (n=1)	1	0
	4C (n=0)	0	0
	5 (n=0)	0	0
4A (n=39)	3 (n=3)	3	0
	4A (n=15)	15	0
	4B (n=11)	9	2
	4C (n=7)	3	4
	5 (n=3)	2	1
4B (n=28)	3 (n=0)	0	0
	4A (n=3)	3	0
	4B (n=8)	5	3
	4C (n=14)	9	5
	5 (n=3)	3	0
4C (n=13)	3 (n=0)	0	0
	4A (n=0)	0	0
	4B (n=1)	0	1
	4C (n=6)	5	1
	5 (n=6)	3	3
5 (n=4)	3 (n=0)	0	0
	4A (n=0)	0	0
	4B (n=0)	0	0
	4C (n=1)	1	0
	5 (n=3)	1	2

BI-RADS, Breast Imaging Reporting and Data System; CEUS, contrast-enhanced ultrasound; DCIS, ductal carcinoma in situ; DCISM, ductal carcinoma in situ with microinvasion.

identification of calcifications (25), the ability to visualize calcifications on sonography has been described (26). Other studies have found a higher frequency of microcalcifications only at imaging for DCISM lesions. Vieira *et al.* (27) found that a mass was detected by mammography or US in over 90% of DCISM patients, which is different from that of DCIS patients. Our findings are similar to those of Wang *et al.* (28), suggesting that the presence of calcifications on sonography may indicate DCISM.

In this study, three enhancement patterns were significantly different between DCIS and DCISM, which included enhancement margin, enlargement of mode, and enlargement of scope. About 47.8% (11/23) of the DCISM lesions showed blurred margin, whereas 24.2% (16/66) of the DCIS lesions showed blurred margin. This aligns with the fact that DCISM is characterized by some degree of invasiveness. The present study found that DCISM lesions are more often characterized by uneven internal perfusion

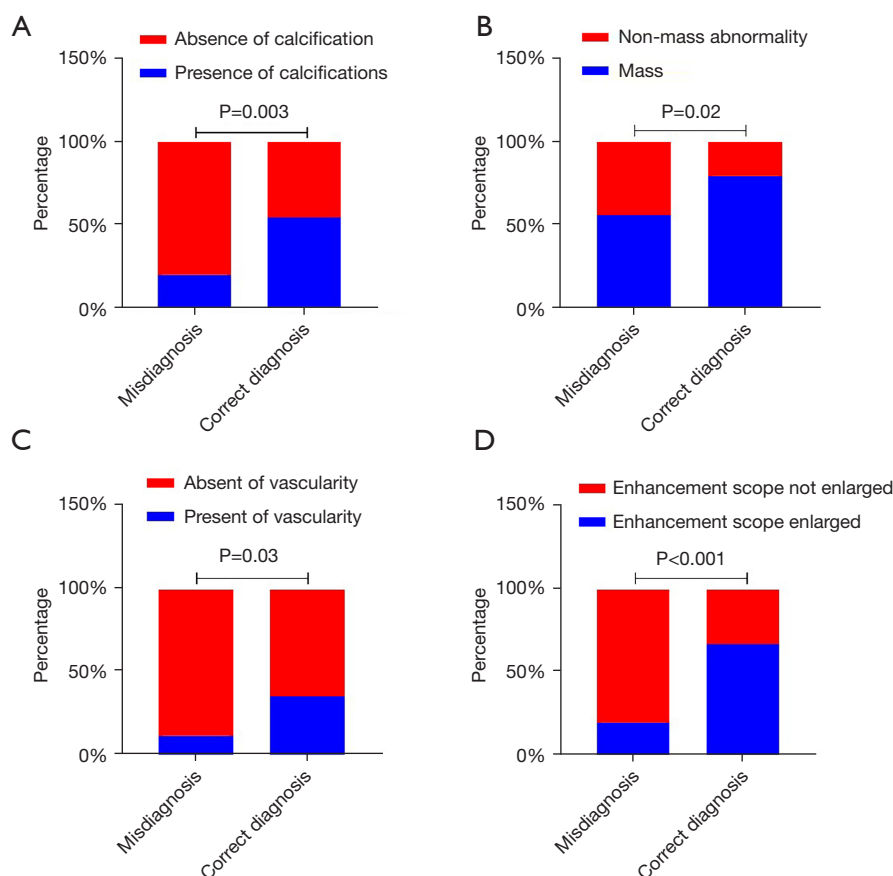


Figure 5 Statistically significant parameters in misdiagnosed and correctly diagnosed cases. (A) Percentage of cases with absence and presence of calcification. (B) Percentage of cases with non-mass and mass abnormalities. (C) Percentage of cases with absence and presence of vascularity. (D) Percentage of cases with unchanged and enlarged enhancement scope.

than pure DCIS lesions, probably due to the rapid growth of DCISM tumor cells. Their interior is prone to necrosis or liquefaction, and the presence of a large amount of fibrosclerotic tissue in the tumor itself leads to a poor blood supply within the lesion (29). Malignant tumors secrete large amounts of vascular endothelial growth factor, which promotes the formation of micro vessels around and within the tumor. This may lead to an increase in the range of enhancement in CEUS. In the present study, we found that DCISM had a higher pathologic grade compared to DCIS, and ER-negative, PR-negative, HER2-positive, and Ki-67-positive were also more frequent than in DCIS, which is the same as the results of previous studies (28,30,31). We investigated the imaging characteristics of DCIS and DCISM lesions on conventional US and CEUS. Eleven statistically significant parameters were identified by univariate analysis. Further multivariate logistic regression

analysis revealed statistically significant differences in two of the parameters (pathologic grading and enhancement range). Based on these two characteristics, a predictive model to assess the likelihood of DCISM was developed. The diagnostic sensitivity and specificity of the model were 87.0% and 81.8%, respectively. The area under the ROC curve for the predictive model was 0.892 (95% CI: 0.824–0.959).

In our study, 44 lesions were categorized as BI-RADS 3-4A. Of these, 22 remained unchanged after CEUS rerating, and 22 were upgraded. However, 3 cases were downgraded from the original BI-RADS 4B to the BI-RADS 4A after CEUS assessment. It is evident that incorporating CEUS in the rerated BI-RADS can improve the efficacy of US in diagnosis breast lesions. A total of 25 cases of malignant lesions were misdiagnosed before surgery. Among these, 24 had pathologic findings indicative of DCIS and 1 had pathologic findings

indicative of DCISM. Non-calcified DCIS may present as a mammography occult palpable lesion, cause for nipple discharge, abnormality in screening US, or finding in the evaluation of disease extent. DCIS detected by US alone is often localized and of low grade, whereas calcified DCIS is more commonly high grade (32). In our study, 20 of the 25 misdiagnosed cases lacked calcification features. Calcifications seen at US are more than three times more likely to be malignant than those not seen in US (33). Even if no calcifications are found within the mass, vigilance should not be relaxed. Ueno (34) was the first to categorize echogenic images of breast disease into “non-tumor image-forming type” (non-mass abnormalities) and “tumor image-forming type” (masses). Non-mass-like breast cancer lesions lack local structural change with an obvious space occupying effect in two different scan directions, and the absence of imaging features on ultrasonography makes them more challenging to diagnose, leading to a relatively high rate of false diagnosis. Our study concluded that of the 64 correctly diagnosed cases, 13 were non-mass like lesions; of the 25 misdiagnosed cases, 11 were non-mass-like lesions, and the difference was statistically significant. Therefore, in dense breast tissue, US can be combined with other diagnostic methods to improve the diagnostic yield. Among the CEUS related BI-RADS score 3-4A malignant lesions, 22 showed a lack of vascularity. The growth of small malignant lesions depends on a normal surrounding capillary network, without the formation of malformed vessels (35). Failure to detect malformed vessels can lead to an erroneous diagnosis of non-malignancy. Most malignant breast lesions show an enlarged range of enhancement using CEUS than using US, while most benign lesions do not (36). However, the range of enhancement was not enlarged in 20 misdiagnosed malignant lesions in our study. It is important to note that most lesions in the modified category were based on lesions without enhancement. Zhang *et al.* (37), reached a similar conclusion that the enlargement after enhancement improved the sensitivity and decreased the negative likelihood ratio (from 0.33 to 0.25) for the diagnosis of malignancy but did not improve the specificity.

There are some limitations in this study. First, it was a retrospective study with a limited sample size. The DCISM groups had few cases, which might affect the statistical conclusions. However, this study is an exploratory study, and the results of the indicator characteristics are considered reliable when compared to those of similar studies. Second, we did not consider the distribution and

degree of vascularization, and three-color Doppler indices (peak systolic velocity, pulsatility index, and resistive index). Third, the observation of sonographic enhancement features is subjective. Therefore, CEUS imaging should be quantitatively evaluated using an objective method to confirm our results.

Conclusions

Understanding the CEUS and clinicopathologic features of DCISM lesions may alert clinicians to the possibility of microinvasion and guide appropriate management.

Acknowledgments

Funding: This work was supported by the National Natural Science Foundation of China (No. 82071925), The Military Logistics Research Project (No. 2022HQZZ02), and the National Natural Science Foundation of China (No. 82371972).

Footnote

Reporting Checklist: The authors have completed the STARD reporting checklist. Available at <https://gs.amegroups.com/article/view/10.21037/gS-24-211/rc>

Data Sharing Statement: Available at <https://gs.amegroups.com/article/view/10.21037/gS-24-211/dss>

Peer Review File: Available at <https://gs.amegroups.com/article/view/10.21037/gS-24-211/prf>

Conflicts of Interest: All authors have completed the ICMJE uniform disclosure form (available at <https://gs.amegroups.com/article/view/10.21037/gS-24-211/coif>). The authors have no conflicts of interest to declare.

Ethical Statement: The authors are accountable for all aspects of the work in ensuring that questions related to the accuracy or integrity of any part of the work are appropriately investigated and resolved. The study was conducted in accordance with the Declaration of Helsinki (as revised in 2013). The study was a retrospective clinical diagnostic test, approved by the Ethics Committee of the Chinese PLA General Hospital (No. S2020-354-01). Informed consent was waived because of the retrospective

nature of the study.

Open Access Statement: This is an Open Access article distributed in accordance with the Creative Commons Attribution-NonCommercial-NoDerivs 4.0 International License (CC BY-NC-ND 4.0), which permits the non-commercial replication and distribution of the article with the strict proviso that no changes or edits are made and the original work is properly cited (including links to both the formal publication through the relevant DOI and the license). See: <https://creativecommons.org/licenses/by-nc-nd/4.0/>.

References

- Jatoi I, Shaaban AM, Jou E, et al. The Biology and Management of Ductal Carcinoma in Situ of the Breast. *Curr Probl Surg* 2023;60:101361.
- Udayasiri RI, Luo T, Gorringer KL, et al. Identifying recurrences and metastasis after ductal carcinoma in situ (DCIS) of the breast. *Histopathology* 2023;82:106-18.
- Champion CD, Ren Y, Thomas SM, et al. DCIS with Microinvasion: Is It In Situ or Invasive Disease? *Ann Surg Oncol* 2019;26:3124-32.
- Wang W, Zhu W, Du F, et al. The Demographic Features, Clinicopathological Characteristics and Cancer-specific Outcomes for Patients with Microinvasive Breast Cancer: A SEER Database Analysis. *Sci Rep* 2017;7:42045.
- Grimm LJ, Ryser MD, Partridge AH, et al. Surgical Upstaging Rates for Vacuum Assisted Biopsy Proven DCIS: Implications for Active Surveillance Trials. *Ann Surg Oncol* 2017;24:3534-40.
- Chin-Lenn L, Mack LA, Temple W, et al. Predictors of treatment with mastectomy, use of sentinel lymph node biopsy and upstaging to invasive cancer in patients diagnosed with breast ductal carcinoma in situ (DCIS) on core biopsy. *Ann Surg Oncol* 2014;21:66-73.
- Chavez de Paz Villanueva C, Bonev V, Senthil M, et al. Factors Associated With Underestimation of Invasive Cancer in Patients With Ductal Carcinoma In Situ: Precautions for Active Surveillance. *JAMA Surg* 2017;152:1007-14.
- Liu H, Zhan H, Sun D, et al. Comparison of BSGI, MRI, mammography, and ultrasound for the diagnosis of breast lesions and their correlations with specific molecular subtypes in Chinese women. *BMC Med Imaging* 2020;20:98.
- Zhu M, Pi Y, Jiang Z, et al. Application of deep learning to identify ductal carcinoma in situ and microinvasion of the breast using ultrasound imaging. *Quant Imaging Med Surg* 2022;12:4633-46.
- D'Orsi CJ, Sickles EA, Mendelson EB, et al. ACR BI-RADS Atlas: Breast Imaging Reporting and Data System. American College of Radiology, Reston, VA, USA. 2013.
- Wang Y, Fan W, Zhao S, et al. Qualitative, quantitative and combination score systems in differential diagnosis of breast lesions by contrast-enhanced ultrasound. *Eur J Radiol* 2016;85:48-54.
- Wan C, Du J, Fang H, et al. Evaluation of breast lesions by contrast enhanced ultrasound: qualitative and quantitative analysis. *Eur J Radiol* 2012;81:e444-50.
- Xia HS, Wang X, Ding H, et al. Papillary breast lesions on contrast-enhanced ultrasound: morphological enhancement patterns and diagnostic strategy. *Eur Radiol* 2014;24:3178-90.
- Xiao X, Dong L, Jiang Q, et al. Incorporating Contrast-Enhanced Ultrasound into the BI-RADS Scoring System Improves Accuracy in Breast Tumor Diagnosis: A Preliminary Study in China. *Ultrasound Med Biol* 2016;42:2630-8.
- Hammond ME, Hayes DF, Dowsett M, et al. American Society of Clinical Oncology/College of American Pathologists guideline recommendations for immunohistochemical testing of estrogen and progesterone receptors in breast cancer (unabridged version). *Arch Pathol Lab Med* 2010;134:e48-72.
- Penault-Llorca F, André F, Sagan C, et al. Ki67 expression and docetaxel efficacy in patients with estrogen receptor-positive breast cancer. *J Clin Oncol* 2009;27:2809-15.
- Bychkovsky BL, Myers S, Warren LEG, et al. Ductal Carcinoma In Situ. *Hematol Oncol Clin North Am* 2024;38:831-49.
- Bonev VV. Ductal carcinoma in situ: a comprehensive review on current and future management for the surgeon and non-surgeon. *AME Surg J* 2021;1:27.
- O'Keefe TJ, Harismendy O, Wallace AM. Histopathological growth distribution of ductal carcinoma in situ: tumor size is not "one size fits all". *Gland Surg* 2022;11:307-18.
- Zhao MR, Ma WJ, Song XC, et al. Feasibility analysis of magnetic resonance imaging-based radiomics features for preoperative prediction of nuclear grading of ductal carcinoma in situ. *Gland Surg* 2023;12:1209-23.
- Delaloge S, Khan SA, Wesseling J, et al. Ductal carcinoma in situ of the breast: finding the balance between overtreatment and undertreatment. *Lancet* 2024;403:2734-46.

22. Giuliano AE, Connolly JL, Edge SB, et al. Breast Cancer-Major changes in the American Joint Committee on Cancer eighth edition cancer staging manual. *CA Cancer J Clin* 2017;67:290-303.
23. Kuerer HM, Smith BD, Chavez-MacGregor M, et al. DCIS Margins and Breast Conservation: MD Anderson Cancer Center Multidisciplinary Practice Guidelines and Outcomes. *J Cancer* 2017;8:2653-62.
24. Jin ZQ, Lin MY, Hao WQ, et al. Diagnostic evaluation of ductal carcinoma in situ of the breast: ultrasonographic, mammographic and histopathologic correlations. *Ultrasound Med Biol* 2015;41:47-55.
25. Rauch GM, Kuerer HM, Scoggins ME, et al. Clinicopathologic, mammographic, and sonographic features in 1,187 patients with pure ductal carcinoma in situ of the breast by estrogen receptor status. *Breast Cancer Res Treat* 2013;139:639-47.
26. Watanabe T, Yamaguchi T, Tsunoda H, et al. Ultrasound Image Classification of Ductal Carcinoma In Situ (DCIS) of the Breast: Analysis of 705 DCIS Lesions. *Ultrasound Med Biol* 2017;43:918-25.
27. Vieira CC, Mercado CL, Cangiarella JF, et al. Microinvasive ductal carcinoma in situ: clinical presentation, imaging features, pathologic findings, and outcome. *Eur J Radiol* 2010;73:102-7.
28. Wang H, Lin J, Lai J, et al. Imaging features that distinguish pure ductal carcinoma in situ (DCIS) from DCIS with microinvasion. *Mol Clin Oncol* 2019;11:313-9.
29. Hanby AM. The pathology of breast cancer and the role of the histopathology laboratory. *Clin Oncol (R Coll Radiol)* 2005;17:234-9.
30. Yao JJ, Zhan WW, Chen M, et al. Sonographic Features of Ductal Carcinoma In Situ of the Breast With Microinvasion: Correlation With Clinicopathologic Findings and Biomarkers. *J Ultrasound Med* 2015;34:1761-8.
31. Ozkan-Gurdal S, Cabioglu N, Ozcinar B, et al. Factors predicting microinvasion in Ductal Carcinoma in situ. *Asian Pac J Cancer Prev* 2014;15:55-60.
32. Izumori A, Takebe K, Sato A. Ultrasound findings and histological features of ductal carcinoma in situ detected by ultrasound examination alone. *Breast Cancer* 2010;17:136-41.
33. Soo MS, Baker JA, Rosen EL. Sonographic detection and sonographically guided biopsy of breast microcalcifications. *AJR Am J Roentgenol* 2003;180:941-8.
34. Ueno E. Classification and diagnostic criteria in breast echography. *Jpn J Medical Ultrasonics* 1986;13:19-31.
35. Weidner N, Semple JP, Welch WR, et al. Tumor angiogenesis and metastasis--correlation in invasive breast carcinoma. *N Engl J Med* 1991;324:1-8.
36. Tian Y, Wang W, Hu Y, et al. The Size Differences of Breast Cancer and Benign Tumors Measured by Two-Dimensional Ultrasound and Contrast-Enhanced Ultrasound. *J Ultrasound Med* 2024;43:1245-50.
37. Zhang JX, Cai LS, Chen L, et al. CEUS helps to rerate small breast tumors of BI-RADS category 3 and category 4. *Biomed Res Int* 2014;2014:572532.

Cite this article as: Jiang Y, Li JK, Huang SS, Li SY, Niu RL, Fu NQ, Wang ZL. The diagnostic value of contrast-enhanced ultrasound combined with clinicopathological features in microinvasive ductal carcinoma *in situ*. *Gland Surg* 2024;13(11):1894-1906. doi: 10.21037/gS-24-211